# First-order autocorrelations and domain-model mode structure of a synchronously pumped mode-locked dye laser

M. De Mazière,* A. Bouwen, and D. Schoemaker

*Department of Physics, University of Antwerp, B-2610 Wilrijk-Antwerpen, Belgium*

Received February 24, 1989; accepted August 24, 1989

First-order field autocorrelation measurements of high dynamic range and sensitivity have been performed on the pulse train of a synchronously pumped mode-locked dye laser with a two-plate birefringent filter as a tuning element. A double-phase-modulation detection technique developed by us for time-resolved stimulated Raman gain spectroscopy was employed. These measurements yield information about the mode structure of the dye-laser pulses. Our experimental results lend support to the domain model as a viable description of the mode structure of imperfect mode locking. Moreover, second-harmonic autocorrelation and cross-correlation widths and shapes are shown to be reconcilable with this model.

## 1. INTRODUCTION

The transform-limited behavior of the pulses of synchronously pumped mode-locked dye lasers is often studied; in particular, the substructure or fluctuations in shape or widths are investigated. It now is generally recognized that the transform limit is not attained if the dye laser is tuned with a two-plate birefringent Lyot filter.

For the investigation of picosecond pulses several techniques are in use. These techniques differ from one another not only by their time resolution and sensitivity, but also by their intrinsic information content. A streak camera can display the pulse profile directly in the time domain, but such cameras are expensive and their time resolution has been lowered to the subpicosecond regime only very recently. Therefore the pulses are examined mostly with the help of autocorrelation profiles. The information that these profiles give depends on the order of the autocorrelation function. The pulses can also be examined in the frequency domain. However, conclusions drawn from these different techniques show ambiguities. Therefore we have performed simultaneous measurements of the first- and second-order autocorrelation profiles and of the spectral shape of a pulse, and we have looked for an interpretation that is consistent with all these diagnostics. We have found that the domain model that has been introduced by Picard and Schweitzer[1] for describing a deviation from perfect mode-locked conditions in terms of the dye-laser mode structure reproduces the essential features of our observations.

An additional motivation for this study was the need for a realistic pulse model that enables us to explain the observed characteristics of picosecond time-resolved stimulated Raman gain (TRSRG) measurements.[2] It is shown in Ref. 2 that the introduction of the domain model for the dye-laser mode structure allows us to simulate the dephasing measurements on liquid test samples of $CS_2$ and $C_6H_6$, whereas, for example, a smooth Gaussian pulse profile does not. This too confirms the interpretations given in this paper.

It is also in connection with the TRSRG experiments that we prefer the first-order autocorrelation profiles to a spectral analysis, although in principle both offer identical information. Indeed, the first-order autocorrelation traces are generated in time-resolved interference (TRIF) measurements, for which the experimental arrangement is automatically included in that for TRSRG measurements. In contrast, additional instrumentation is needed for a spectral analysis. Moreover, the former technique delivers results directly in the time domain, whereas the latter one requires an additional Fourier transformation procedure. Furthermore, the TRIF measurements make use of the double-phase-modulation technique developed by us for picosecond TRSRG experiments[3,4] and time-resolved induced optical transparency effects.[5] As a result, the TRIF technique has a much higher sensitivity and dynamic range ($\simeq 10^3$) in comparison with the well-known second-harmonic second-order autocorrelation technique (Section 2). This feature enables it to establish the occurrence of domain-model substructure and to distinguish its parameters. The second-order autocorrelation trace can be interpreted within the domain model, but it cannot by itself discern its presence unambiguously.

Section 2 outlines the experimental methods. Section 3 discusses the experimental observations, together with their analysis in terms of the domain model. Principal conclusions are summarized in Section 4.

## 2. EXPERIMENTAL ARRANGEMENT

### A. Laser Configuration

The laser system to which the pulse analysis refers is a Spectra-Physics synchronously pumped mode-locked dye-laser system. The pump laser is a mode-locked argon-ion laser (514.5 nm) emitting an 82.3-MHz pulse train of 700-mW average mode-locked power. Pulse widths, as read directly on a Tektronix sampling oscilloscope, are ~190 psec. The synchronously pumped dye laser is a Rhodamine-6G dye laser, with a two-plate birefringent Lyot filter in the cavity. When pumped by half the pump power, i.e., by ~350 mW average, and length-tuned to optimum mode-locked performance, its average output power is near 30 mW.

0740-3224/89/122370-06$02.00 

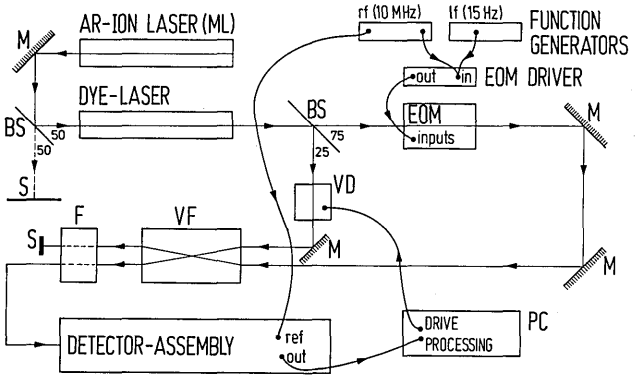


Fig. 1. Block diagram of the TRIF setup for measuring the first-order autocorrelation traces. ML, mode-locked; EOM, electro-optic modulator; PC, personal computer; M, mirror; BS, beam splitter; S, beam stop; F, spatial filtering system; VF, variable-focusing system; VD, variable-delay line.

### B. Time-Resolved Interference Setup

The TRIF measurements require the dye-laser beam to be split by a beam splitter into two replicas that can be variably delayed relative to each other, effectively making up two branches of an interferometer. Both branches propagate in parallel to the detector assembly, the delayed one being caught by it. A simplified block diagram of the setup is given in Fig. 1.

The variable focusing block refers to a set of two identical lenses, between which both beam replicas are focused together to the same point. The second lens is also positioned near the focal distance ($f \simeq 30$ mm) from the focal point and hence serves for recollimation of both beams. This setup derives immediately from that for the picosecond TRSRG measurements.[3,4] We detect the interference term that arises from admixing a portion of the modulated beam in the detected beam. This portion is controlled through slight readjustments on the positioning of the second lens.

Even a minimal interference contribution is detectable as a result of the double-phase-modulation technique[3,4] that is used. This technique uses both an rf (~10 MHz) and an appropriate low-frequency (~15-Hz) electro-optic phase modulation (Coherent electro-optic modulator Model 3025) of the fixed-delay branch, with corresponding rf lock-in-amplifier synchronous detection followed by low-frequency rms voltmeter detection. The detector assembly contains an EG&G FND-100 Si photodiode and narrow-band amplifier tuned to the rf modulation frequency. The rms voltmeter output is converted from a voltage to a frequency and processed by a personal computer synchronously with the delay scan. The latter is driven by a stepper motor that is steered by the personal computer.

The interference signal carries the first-order field autocorrelation function. The signal is discriminated against the background of the unmodulated beam, and phase noise is eliminated through the use of the double-phase-modulation detection technique.[3,4] The utmost care is taken to reduce the contributions from the stray light of the directly modulated fixed branch so that this one induces no signal on its own.

Thus a registration of the interference signal during a scan of the delay $t_D$ effectively traces the first-order field autocorrelation function $G^{(1)}(t_D)$. In a comparative series of scans as a function of the mode-locking parameters, all other experimental variables (spatial alignment, focusing, ...) are kept fixed, for it is evident that a systematic dependence on them cannot be retraced.

### C. Other Pulse-Train Diagnostics Methods for Comparison

The other diagnostics methods are (1) spectral bandwidth measurements [i.e., spectrally resolved interference (SRIF) measurements] by means of a scanning interferometer, having a free spectral range of 300 GHz and a spectral resolution better than 6 GHz (Spectra-Physics Models 410-05 and 476), and (2) continuous monitorings of second-harmonic, second-order intensity autocorrelation traces without background (Spectra-Physics autocorrelator Model 409). The latter $XY$ recordings are read out from a Gould digital storage oscilloscope.

All three diagnostics measurements are carried out in parallel. Our assessment of the latter two is guided by comparisons with point-by-point recordings of second-harmonic autocorrelation traces with background that were recorded beforehand.[6]

## 3. INTERPRETATION OF THE DIAGNOSTICS OBSERVATIONS

We now turn to the characteristics of our experimental results and their interpretation in terms of the domain model for the dye-laser mode structure.

Figure 2 presents representative traces that have been recorded under optimal dye-laser mode-locked conditions, as is confirmed by the correspondingly observed narrow, smooth second-harmonic second-order autocorrelation profile. Nevertheless, pronounced wiggles show up in the TRIF curve, and the SRIF spectrum is clearly structured. The TRIF wiggles exhibit some periodicity that cannot be related in any way to the fundamental beat frequency between the laser modes, i.e., the mode-locking frequency $\Gamma = 82.3$ MHz. Moreover, with changes in the dye-laser cavity length

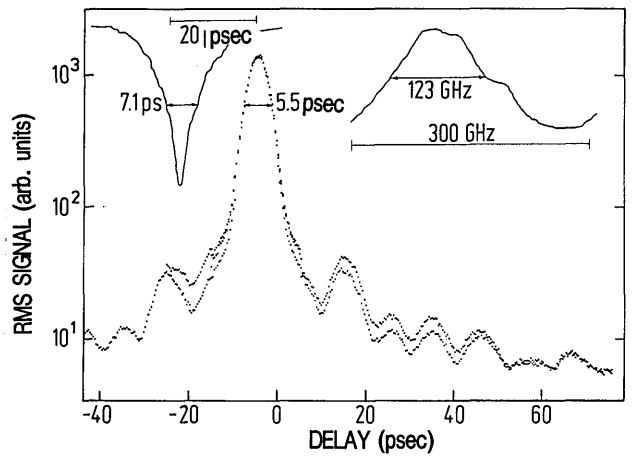


Fig. 2. Logarithmic plot of the experimental TRIF trace under optimum dye-laser tuning conditions. The quasi-simultaneously registrated intensity autocorrelation trace and spectral-bandwidth curves are included in the upper left and upper right-hand corners, respectively.

or ion-pump-laser conditions, one readily observes alterations in the resolution as well as in the exact positions and shapes of the wiggles. These changes are so small that the second-harmonic, second-order autocorrelation trace remains unchanged to the eye. Simultaneously, the SRIF structure is seen to be altered.

The above observations suggest that substructure exists in the dye-laser pulses, which reveals itself in particular in the TRIF curves. The adoption of the domain model for the dye-laser mode structure has enabled us to identify the main characteristics of the experimental observations.

Hereafter, the fundamentals of the domain model are reviewed. Only those essentials will be kept that are required for deriving the shapes of the recorded correlation traces in Subsections 3.A and 3.B. This fact should be kept in mind in subsequent discussions and especially in attempting closer comparisons with experimental data (Subsection 3.C).

According to the domain model, the whole of the oscillating modes, $N_{\text{tot}}$, is subdivided into $M$ coexisting domains slightly shifted with respect to one another instead of being all locked together uniformly. Each domain ($m$) individually is a perfectly mode-locked set of $N_m$ adjacent modes centered at a frequency $\nu_m \equiv \nu + \delta_m$ and locked at the intermode separation $\Gamma_m$. $N_m$ and $M$ differ by ~2 orders of magnitude ($N_m \gg M$) and are both assumed to be odd. The latter assumption is made solely for the purpose of mathematical notation; therefore it will be dropped when experimental results are simulated (Subsection 3.C). Thus one may write

$$N_{\text{tot}} = \sum_{m=-\frac{M-1}{2}}^{m=+\frac{M-1}{2}} N_m. \tag{1}$$

For more details about the model, refer to the original paper.[1]

We assume all $\Gamma_m$ to be equal to the pump mode-locking frequency $\Gamma$ and all domains to have mutually the same numerical parameters (e.g., $N_m \equiv N$) except for their center frequencies. The latter are taken equally spaced:

$$\nu_m = \nu + m\delta, \tag{2}$$

with the restriction that $\delta$ differs from the intermode separation $\Gamma$ by ~2 orders of magnitude and is no integral multiple of $\Gamma$.

The fully coherent field within one domain is the well-known phase-locked superposition of the $N$ fundamental modes in the domain. It may also be treated as a slowly varying, e.g., Gaussian, supermode $\varepsilon(t)$ of width (FWHM) $\sqrt{2}t_p \simeq \sqrt{6}/\pi N\Gamma$.

### A. First-Order Correlations

The signal $\mathcal{S}'(t_D)$ measured in the TRIF experiments in a double-phase-modulation configuration looks like

$$\mathcal{S}'(t_D) \propto 2\sqrt{a}\,\text{Re}\int \mathrm{d}t\, E(t)E^*(t - t_D) \times \exp[i(\varphi - \varphi' - 2\pi\nu t_D - \alpha)]. \tag{3}$$

$\sqrt{a}E(t - t_D)$ is the delayed (over $t_D$) and attenuated [$\sqrt{a}$ $\exp(i\alpha)$] replica of the total pump field amplitude $E(t)$ of frequency $\nu$; $\varphi'$ and $\varphi$ are their respective phases, considered constants during a pulse. We recall that $\varphi$ is modulated from the outside. We will drop the factor $2\sqrt{a}$ from here on.

The signal $\mathcal{S}(t_D)$, obtained through double lock-in processing of $\mathcal{S}'(t_D)$, is proportional to the modulus of the first-order field autocorrelation function $G^{(1)}(t_D)$:

$$\mathcal{S}(t_D) \propto \left|\int \mathrm{d}t E(t)E^*(t - t_D)\right|. \tag{4}$$

The integration extends over many (~50) periods of the pulse train. Therefore upon insertion into relation (4) of the domain-structure Eqs. (1) and (2), i.e., of

$$E(t)\exp[-i(2\pi\nu t)] = \frac{1}{M}\sum_{m=-\frac{M-1}{2}}^{m=+\frac{M-1}{2}} \varepsilon(t)\exp[-i(2\pi\nu_m t + \varphi)], \tag{5}$$

with $\nu_m \equiv \nu + \delta_m$, one sees that terms originating in the correlation among different domains vanish. One then finds that

$$\begin{aligned}\mathcal{S}(t_D) &\propto \left|\frac{1}{M^2}\sum_{m=-\frac{M-1}{2}}^{m=+\frac{M-1}{2}} \int \mathrm{d}t\varepsilon(t)\varepsilon^*(t - t_D)\exp(-i2\pi\delta_m t_D)\right| \\ &\propto \left|\int \mathrm{d}t\varepsilon(t)\varepsilon^*(t - t_D)\right| \\ &\quad \times \frac{1}{M}\left|\frac{1}{M}\sum_{m=-\frac{M-1}{2}}^{m=+\frac{M-1}{2}} \exp(-i2\pi\delta_m t_D)\right|.\end{aligned} \tag{6}$$

$\varepsilon(t)$ points to the supermode amplitude. The integral can be confined to one pulse period; however, for pulse widths of ~10 psec this is about equivalent to extending the limits to infinity.

The result is proportional to $|U(t_D)|$, the modulus of the visibility curve for the ideally mode-locked pulse within one domain, modulated by the modulus of the visibility curve due to the domain structure, indicated below as $|V(t_D)|$ or domain visibility. The concept visibility curve $U(t_D)$ refers to the envelope of $G^{(1)}(t_D)$.[7]

With the assumption of Eq. (2) one finally obtains

$$\mathcal{S}(t_D) \propto \left|\int \mathrm{d}t\varepsilon(t)\varepsilon^*(t - t_D)\right| \times \frac{1}{M}\left|\frac{\sin(M\pi t_D\delta)}{M\sin(\pi t_D\delta)}\right|, \tag{7}$$

which is written as

$$\mathcal{S}(t_D) \propto \frac{1}{N}|U(t_D)| \times \frac{1}{M}|V(t_D)|. \tag{8}$$

$V(t_D)$ has the same structure as $U(t_D)$. Its oscillatory period is $1/M\delta$ instead of $1/N\Gamma$, by which its FWHM is reduced to two times the coherence time, $2t_c \simeq 2\sqrt{3}/\pi M\delta$, instead of two times the pulse width, $2t_p \simeq 2\sqrt{3}/\pi N\Gamma$. Furthermore, its repetition period is $1/\delta$ rather than $1/\Gamma$ ($1/\delta \ll 1/\Gamma$). If a Gaussian-envelope approximation is made for $\varepsilon(t)$, of width $\sqrt{2}t_p$, $U(t_D)$ is also a Gaussian of width $2t_p$ (FWHM).

## B. Second-Order Correlations

### 1. *Autocorrelations*

The analogous expression for the second-harmonic, second-order autocorrelation function, with incorporation of the domain model, is not identical to the previous one squared [relations (7) and (8)] but nevertheless bears resemblance to it.[1] However, since no details of its structure are detected experimentally, the structure is not explicated here. One important feature of the second-harmonic autocorrelation trace to be remembered is that the central single pulse of the ideally mode-locked case consists of a sharp central coherence peak and a weaker broadened base.[1] Further discussions of this subject are given in Subsection 3.C.

### 2. *Cross Correlations*

In order to characterize the performance of a double synchronously pumped mode-locked dye-laser system, the sum-frequency cross correlation between the two dye lasers, denoted $L$ and $S$, adds important diagnostic information. Therefore we trace the effect of incorporating the domain model into the expression for the sum-frequency cross-correlation curve. The latter reads as

$$G_{L,S}(t_D) \propto \int_{-\infty}^{+\infty} dt |E_L(t)E_S(t-t_D)|^2 \propto \int_{-\infty}^{+\infty} dt I_L(t)I_S(t-t_D). \tag{9}$$

Now the domain structure Eq. (5) is inserted into $E_L$ and $E_S$, supplementing the descriptive parameters $N$, $M$, and $\delta$ with the subscripts $L$ and $S$, respectively. Of course $\Gamma$ is fixed for it is determined by the common pump laser. Relation (9) becomes

$$\begin{aligned} G_{L,S}(t_D) \propto & \frac{1}{N_L{}^2} \sum_{n_L,n_L'=-\frac{N_L-1}{2}}^{n_L,n_L'=+\frac{N_L-1}{2}} \frac{1}{N_S{}^2} \sum_{n_S,n_S'=-\frac{N_S-1}{2}}^{n_S,n_S'=+\frac{N_S-1}{2}} \frac{1}{M_L{}^2} \\ & \times \sum_{m_L,m_L'=-\frac{M_L-1}{2}}^{m_L,m_L'=+\frac{M_L-1}{2}} \frac{1}{M_S{}^2} \sum_{m_S,m_S'=-\frac{M_S-1}{2}}^{m_S,m_S'=+\frac{M_S-1}{2}} \\ & \times \exp[2\pi i(n_S - n_S')\Gamma t_D]\exp[2\pi i(m_S - m_S')\delta_s t_D] \\ & \times \int_{-\infty}^{+\infty} dt(\exp\{-2\pi i[(n_L - n_L') + (n_S - n_S')]\Gamma t\} \\ & \times \exp\{-2\pi i[(m_L - m_L')\delta_L + (m_S - m_S')\delta_S]t\}) \times |E_L|^2|E_S|^2 \end{aligned} \tag{10}$$

on the assumption that both dye-laser pulses are located at $t = 0$. Here $E_L/N_LM_L$ and $E_S/N_SM_S$ now stand for the mode amplitudes.

Formally this expression looks completely similar to that for the intensity autocorrelation (along the same domain model).[1] However, the cross correlation contrasts with the autocorrelation in that it correlates two lasers of mutually independent substructures. One cannot expect any matching between the domains of the $L$ and $S$ dye lasers. Therefore the cross-correlation trace cannot display the coherence peak, which in the autocorrelation arises through the exact matching of domains. The cross correlation only preserves the broad base. This conclusion follows equally from developing relation (10). The fourfold sum is reduced to (schematically)

$$\begin{aligned} G_{L,S}(t_D) \propto & \frac{1}{M_L{}^2} \sum_{m_L=-\frac{M_L-1}{2}}^{m_L=+\frac{M_L-1}{2}} \frac{1}{M_S{}^2} \sum_{m_S=-\frac{M_S-1}{2}}^{m_S=+\frac{M_S-1}{2}} I_{N_L}I_{N_S} \\ & (m_L = m_L',\ m_S = m_S') \\ & \times \Bigg\{ \sum_{n_L=n_L'} \sum_{n_S=n_S'} \qquad (n_L \neq n_S) \\ & + \sum_{n_L=n_S'} \sum_{n_S=n_L'} \exp[-2\pi i(n_L - n_S)\Gamma t_D] \\ & (n_L \neq n_S) \\ & + \sum_{n_S=n_S'=n_L=n_L'} + \sum_{n_S,n_S'} \exp[2\pi i(n_S - n_S')\Gamma t_D] \Bigg\} \\ & (n_L + n_S = n_L' + n_S', \\ & \text{with none of the indices mutually equal}) \end{aligned} \tag{11}$$

and with $I_{N_{L(S)}} \equiv |E_L/N_L|^2(|E_S/N_S|^2) \equiv |E_{N_{L(S)}}|^2$. The sum in brackets corresponds to the autocorrelation trace of an ideally mode-locked laser pulse (if $N_L = N_S$).[1,8]

In other words, the observed cross correlation $G_{L,S}(t_D)$ is the superposition of all domain cross correlations $G_{m_L,m_S}(t_D)$, in which $G_{m_L,m_S}(t_D)$ stands for the cross correlation between the pair of supermodes centered at $\nu_L + m_L\delta_L$ and $\nu_S + m_S\delta_S$, respectively. Each supermode is an ideally mode-locked pulse of width $\propto 1/N_{L(S)}\Gamma$, i.e., approximately the observed pulse-envelope width $t_{p,L(S)}$.

## C. Experimental Results

In our analysis of the experimental results, no attempt is made to fit the data quantitatively. The domain model in its most elementary form is too simple and rigid for that purpose. Moreover the SRIF curves cannot resolve separate modes; they only serve as another indication of the total oscillator bandwidth and of coarse spectral structure. In this connection, it is worth noting from the specifications of the SRIF equipment (Subsection 2.C) that the SRIF spectra encompass neither the time range nor the time resolution of the TRIF curves. Fourier analysis of the spectra has not been performed. In the following discussions, therefore, numerical simulations or parameter values give only indications of a more complex reality.

Returning to Fig. 2, let us first focus on the TRIF wiggles. Identification of this structure with $U(t_D)$ is impossible, if one accounts for the autocorrelation width's being ~7 psec for determining $N$, with $\Gamma$ being 82.3 MHz. In particular, the apparent periodicity is unexplained. However, the latter can be related essentially to the domain structure. This is proved in Fig. 3, in which the main features of Fig. 2 have been generated by evaluating relations (7) and (8) with a

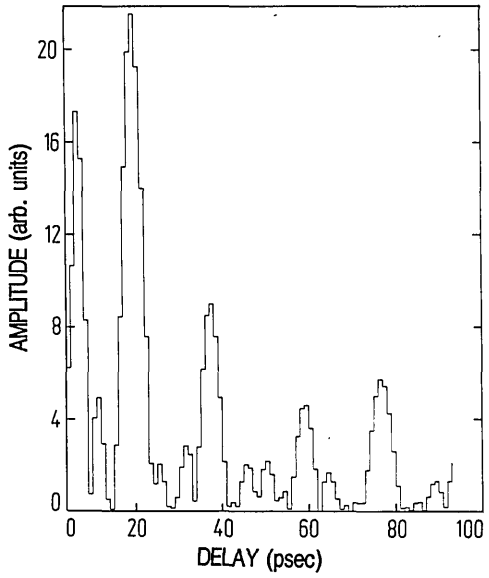


Fig. 3. Numerical evaluation of the TRIF signal based on the domain model [relation (7)], to be compared with Fig. 2. The parameters are $\Gamma = 82.3$ MHz, $N = 875$, $M = 4$, and $\delta = 52$ GHz, corresponding with a second-harmonic second-order autocorrelation envelope width of $\sqrt{2}t_p \sim 10.8$ psec and coherence width of $\sqrt{2}t_c \sim 3.7$ psec. Note the linear vertical scale and the exclusion of the zero-delay point.

suitable set of domain-model parameters. Notice that, for reasons of presentation, the figure starts just on the right of the zero-delay peak, which in the same units would have an amplitude of 100.

The value of $\delta$ (52 GHz) determines the overall repetition period $1/\delta = 19$ psec of $V(t_D)$. Nevertheless the signal strength is attenuated over successive periods by the pulse envelope $U(t_D)$. The larger $N$, the faster the attenuation, which agrees with the tendency to better mode locking. Also, a peak in $V(t_D)$ may be quenched, or cut in two, if it coincides with a minimum in $U(t_D)$. Or else it may be slightly enhanced relative to its following neighbor if it coincides exactly with a maximum in $U(t_D)$. In other words, the nonmonotonical decrease of the wiggles stems from the multiplication of the domain structure $V(t_D)$ with the pulse-envelope structure $U(t_D)$.

This behavior has been observed experimentally. Minimal changes in the dye-laser cavity tuning, which do not visibly alter the observed autocorrelation trace, do induce a structural modification of the SRIF trace, together with small shifts and distortions plus mutual amplitude changes of the TRIF wiggles.

From $\delta$, together with the width of the central peak $2t_c$, $M$ is deduced. It is confirmed that $M\delta$ closely agrees with the observed SRIF width. An almost identical value of $M\delta$ can be produced with a smaller value of $\delta$ and a correspondingly larger value of $M$. These modifications make the SRIF trace sharper with a smoother envelope, as can be expected intuitively.

This feature has been observed equally well experimentally under different operating conditions, e.g., after a realignment of the pump laser. Simultaneously the wiggle structure changes more substantially. As it appears from Figs. 2 and 3 that the TRIF curves reveal little more than the peaks at multiples of $1/\delta$, an enlarged $\delta$ makes only the first secondary peak remain detectable. For example, we often observed[6] a rather smooth TRIF curve, with one clear secondary peak at ~65-psec delay, corresponding with $\delta$ being ~15 GHz. By assuming $M$ equal to ~11, we obtained consistency with the width of the central peak ($2t_c \simeq 6.7$ psec) and that of the SRIF trace ($\simeq$130 GHz). The latter showed a smooth profile.

With regard to the autocorrelation traces, at most only small changes in width or shape are discerned with the previously discussed changes in the TRIF and SRIF curves. To our belief, it is due to their lack of sensitivity in comparison with our TRIF measurements that no detailed structure is distinguishable. Therefore we used a more superficial approximation for the second-order autocorrelation function of substructured pulses in order to check their consistency with our picture:

$$G^{(2)}(t_D) = G_p^{(2)}(t_D)[1 + wG_N^{(2)}(t_D)]. \tag{12}$$

Equation (12) is known as the Pike–Hercher model.[9] Herein $G_p^{(2)}(t_D)$ represents the pulse-envelope autocorrelation function, and $G_N^{(2)}(t_D)$ originates from the deviation from perfect mode locking. A weight $w$ of order 1 is attached to $G_N^{(2)}(t_D)$. The widths of $G_p^{(2)}(t_D)$ and $G_N^{(2)}(t_D)$ are associated with the pulse-envelope width ($t_p$) and the pulse-coherence width ($t_c$), respectively.

We believe that the domain model fits into this approximation, yielding equivalent parameters $t_p$ and $t_c$ but starting from a more elaborate physical picture.[1] We found that a best fit of our experimental autocorrelation traces is always obtained with Eq. (12), with a Gaussian dependence on $t_D$ for both $G_p^{(2)}(t_D)$ and $G_N^{(2)}(t_D)$ and a ratio of $t_c/t_p$ of the order 1/3 to 1/5.[6] This observation supports the domain model as well as the model parameter values discussed by us previously (cf. Figs. 2 and 3).

Some other authors[10,11] have found that the width and the shape of the autocorrelation fit are well fitted with a single exponential. This function yields a FWHM approximately half that of $G_p^{(2)}(t_D)$. These authors have explained these characteristics by taking into account pulse-width variations. However, their assumptions have been doubted already by Fleming *et al.*[12] and McDonald *et al.*[13] We too reject their explanation for two reasons. First, we believe that it rests on a distribution width that is too broad by a factor of 2 to 2.5 by contrast with recent experimental findings of Kluge *et al.*[14] And, second, we believe that the TRIF observations have proved that the domain model provides a more reasonable explanation for the measured autocorrelation profiles.

Our last diagnostics are cross-correlation measurements between the two dye lasers in the double synchronously pumped mode-locked system that we used.

If at first sight the cross-correlation width looks approximately a factor 2 too broad in comparison with the observed autocorrelation widths and the expected amount of jitter between both dye lasers,[6,14,15] it does not in comparison with the pulse-envelope widths, $t_p$, deduced from a fit of the autocorrelation to Eq. (12). This result agrees with what is expected from relation (11). On the contrary, carrying on Van Strijland's assumptions[10] for both dye lasers in a calculation of their cross correlation yields almost equally well the width of the observed trace but not its shape. Here again, the shape obtained from adopting the domain model compares more favorably with the experimental one.

## 4. CONCLUSIONS

Two important conclusions are drawn from this paper.

First, first-order field autocorrelations generated in TRIF measurements by means of our double-phase-modulation detection technique provide an accurate and sensitive probe of the pulse behavior of a cw mode-locked dye laser.

Second, the domain model gives a reasonable description of the mode structure of a Rhodamine-6G synchronously pumped mode-locked dye laser with a two-plate birefringent Lyot filter.

With respect to the first conclusion, the high sensitivity and dynamic range of our measurements ($\simeq 10^3$) allow one, e.g., to assess the criticality of adjusting pump-laser and dye-laser operation parameters or to discover the occurrence of secondary pulses originating in unwanted reflections in the optics (e.g., in beam splitters). They do this far better than conventional second-harmonic, second-order autocorrelation measurements.

As to the second conclusion, the inadequacy of a single diagnostics method for judging a pulse model should be stressed: The combination of the usual diagnostics with our time-resolved interference measurements permits an evaluation of the domain-model parameters if this model is adopted. The results thus obtained have proved to be quite adequate for the analysis of TRSRG experiments.[2,6] The adequacy of these results adds evidence for the applicability of the domain model for the purpose of interpreting experiments that are sensitive to a long-term average over the pulse train.

## ACKNOWLEDGMENTS

The authors want to thank P. Casteels for his invaluable contributions in automating the setup. Discussions with C. Sierens are gratefully acknowledged. M. De Mazière thanks the National Fund of Scientific Research—Belgium for a research assistantship. This research was made possible through financial support from Interuniversitair Instituut voor Kernwetenschappen and the Geconcerteerde Acties (Ministerie voor Wetenschapsbeleid), to which the authors are greatly indebted.

* Present address, the Belgian Institute for Space Aeronomy, Ringlaan 3, B-1180 Brussels, Belgium.

## REFERENCES

1. R. H. Picard and P. Schweitzer, Phys. Rev. A **1**, 1803 (1970).
2. M. De Mazière, C. Sierens, and D. Schoemaker, J. Opt. Soc. Am. B **6**, 2376 (1989).
3. M. De Mazière and D. Schoemaker, J. Appl. Phys. **58**, 1439 (1985).
4. C. Sierens, A. Bouwen, E. Goovaerts, M. De Mazière, and D. Schoemaker, Phys. Rev. A **37**, 4769 (1988).
5. C. Sierens, W. Joosen, and D. Schoemaker, Phys. Rev. B **37**, 3075 (1988).
6. M. De Mazière, Ph.D. dissertation (University of Antwerp, Antwerp, Belgium, 1986).
7. M. V. Klein, *Optics* (Wiley, New York, 1970).
8. S. N. Ketkar, J. W. Keto, and C. H. Holder, Jr., Rev. Sci. Instrum. **52**, 405 (1981).
9. H. A. Pike and M. Hercher, J. Appl. Phys. **41**, 4562 (1970).
10. E. W. Van Strijland, Opt. Commun. **31**, 93 (1979).
11. J. C. Diels, in *Proceedings of the 2nd Symposium on Ultrafast Phenomena in Spectroscopy* (Physikalische Geschellschaft der Deutsche Demokratischer Republik, Berlin, German Democratic Republic, 1980).
12. G. R. Fleming, D. Waldeck, and G. S. Beddard, Nuovo Cimento B **63**, 151 (1980).
13. D. B. McDonald, J. L. Rossel, and G. R. Fleming, IEEE J. Quantum Electron. **QE-17**, 1134 (1981).
14. J. Kluge, D. Wiechert, and D. Von der Linde, Opt. Commun. **51**, 271 (1984).
15. R. K. Jain and J. P. Heritage, Appl. Phys. Lett. **32**, 41 (1978).